Paper ID APEN-MIT-2019_141
Applied Energy Symposium: MIT A+B
May 22-24, 2019 • Boston, USA

Increasing the Accuracy of Initial Feasibility Studies - Utilising Numerical Models to Estimate the LCoE of Floating Tidal Energy Platforms

John McDowell
IDCORE
Sustainable Marine Energy Ltd.
Edinburgh, UK
john.mcdowell@sustainablemarine.com

Penny Jeffcoate
Sustainable Marine Energy Ltd.
Edinburgh, UK
penny.jeffcoate@sustainablemarine.com

Lars Johanning
IDCORE
University of Exeter
Penryn, UK
L.Johanning@exeter.ac.uk

Tom Bruce
IDCORE
University of Edinburgh
Edinburgh, UK
Tom.Bruce@ed.ac.uk

Weichao Shi
IDCORE
University of Strathclyde
Glasgow, UK
weichao.shi@strath.ac.uk

Abstract - This paper utilizes numerical modelling techniques to estimate the MetOcean conditions in regions with potential for tidal energy development. Understanding and incorporating these MetOcean site characteristics into the initial stages of a feasibility study, will increase the accuracy of economic viability predictions. This more comprehensive approach will assist in building investor confidence, as the previously overlooked or unknown lifetime costs can be estimated and included in the choice of ultimate deployment position.

Another advantage of this approach is that it uses freely available data, allowing site assessments to determine project feasibility, without high upfront investment. Freely available astronomic, bathymetric and meteorological data was therefore input into a Delft3D-FM simulation of the Bay of Fundy. Models were calibrated with tide gauge, flowmeter and wave buoy data to output spatially and temporally varying estimates of tidal height, flow velocity and significant wave height.

Results demonstrate that areas of highest resource are the most profitable, but sheltered areas with lower flow speeds are also highly economically viable. For an emerging technology sector with relatively limited operational experience, it is recommended that these areas of less risky investment opportunity should be targeted by tidal energy developers.

Keywords—Floating Tidal Energy, Site Selection, Weather Windows, Numerical Modelling

I. Introduction

The tidal stream sector is on the cusp of technological maturity, with clear convergence of design towards flow-aligning floating/bed-mounted three-bladed horizontal-axis turbines. The challenge for the sector is now to achieve commercial maturity, through a combination of technological improvements for increased efficiency, and procedural improvements for increased economic viability. It is the latter that this paper will focus upon.

Tidal deployment sites are often selected based purely on their potential for power output [1] [2], with the reasoning that a large financial return will offset the relatively high Operations & Maintenance (O&M) lifetime costs. However, the impact of MetOcean site characteristics on these lifetime costs is rarely considered, which generates falsely favourable Levelized Cost of Energy (LCoE) values for high resource sites during initial feasibility studies.

Temporally and spatially varying data is required for an accurate approximation of the constraining effects of MetOcean conditions on marine operation success rates, and the subsequent impact upon project costs. Unfortunately, comprehensive MetOcean data is difficult and costly to attain. This paper builds upon existing work by the authors [3], to further investigate utilizing freely available data and numerical modelling techniques to provide accurate representations of environmental conditions during the early project stages. An improved site selection methodology that incorporates this data into feasibility studies will not only help to minimise early stage project costs, such as superfluous additional resource assessments [4], but also provide quantifiable estimates of regional variations in lifetime costs.

All of the models and sources of data used to generate the results for this study are freely available. The Delft3D-FM suite was selected as a well-documented and user-friendly software package, that is capable of accurately modelling tidal flows, winds and waves concurrently [5], [6]. The resource data for a proposed deployment region/site may be unavailable, costly, or simply non-existent, and therefore models that require a high degree of user input and calibration are not of use at an early project stage. Deciding upon a “best value for money available” ethos mimics the initial position of an informed, but financially restricted tidal energy developer.

The FLOW and WAVE modules of Delft3D-FM were coupled to account for the impacts of wind and waves on the flow, and vice versa the impact of flow and wind on waves. The TPXO 7.2 Global Inverse Tidal Model [7] and GEBCO '08 (General Bathymetric Chart of the Oceans) bathymetry data [8] was used to generate approximations of tidal heights and depth-averaged flow velocities. Wind velocity data was extracted from the DHI MetOcean Data Portal and was used to generate approximations of significant wave heights.

An A-Star Algorithm was utilised to calculate the optimum route between suitable port locations and potential deployment sites within the domain [9]. For each grid cell along the route, Weibull Persistence Statistics were utilised to estimate probabilities of operational MetOcean limit exceedance for the expected duration of transit and operations. This allowed for an estimation of the occurrence of weather windows of a required duration, and the statistically likely waiting times for these weather windows [10]. Costs have been assigned to these waiting times based on previous operational experience at SME and through consultation with marine contractors.

With revenue calculated from annual energy production, and the aforementioned estimates of operational expenditures, it is possible to generate spatially varying LCoE approximations. This will allow a developer to make an informed decision on the optimum deployment location for a tidal energy device, and consequently will facilitate the sector's transition towards commercial maturity.

II. Methodology

A. Case Study Device & Location

The Sustainable Marine Energy Ltd. (SME) floating tidal energy device, PLAT-I (PLATform-Inshore), was used as a case study device in terms of power extraction and operational constraints. PLAT-I is attached to the seabed with SME rock anchors and mooring lines, leading to a flow aligning turret on the bow (Figure 1). The current platform, PLAT-I_4.40 houses four in-stream turbines with a 4m rotor diameter, each with a rated power of 70kW.

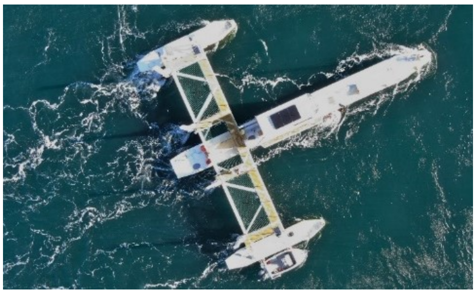

Figure 1. Operational PLAT-I tidal energy device.

The wider Bay of Fundy in Eastern Canada (Figure 2) was selected as a case study location, due to known hotspots of tidal energy and data availability for model validation.

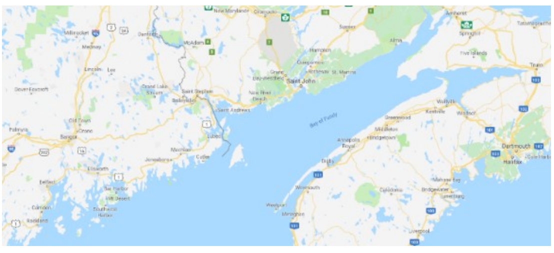

Figure 2. Wider Bay of Fundy area, Eastern Canada.

B. Model Setup

1) Domain

The GEBCO bathymetry data is a continuous high-resolution terrain model generated from the interpolation of multiple databases of satellite data and ship-track soundings. The GEBCO dataset gives up to 20m resolution, which is sufficiently detailed for an initial site assessment, but is also limited in accuracy in areas that are not frequented by vessels, or areas of complex bathymetry. The data was loaded into the Delft3D-FM model using the WGS '84 (World Geodetic System) coordinate and a UTM (Universal Transverse Mercator) Zone 20T chart datum.

A single depth-layer computational grid of 1302x570x1 400m grid cells was generated over the bathymetry, with a time step of 1s used to satisfy the Courant condition [11]. The water temperature and density was set to 8°C and 1025kg/m^3 to represent North Atlantic seawater [5], and a Manning friction coefficient of 0.026 m$^{-1/3}$/s was applied uniformly to represent a deep, rocky bed [12]. Data was output at hourly intervals over a 1-year model duration. All other physical and numerical parameters were left as Delft3D-FM defaults.

Historic Wind Velocity data at 10m above chart datum (W_{10}) for the duration of the simulation was downloaded from the DHI MetOcean Portal [13] at the location of Lighthouse Cove (44.250254, -66.392838). The wind data was applied consistently across the domain but varied in magnitude at hourly intervals (Figure 3). Spatial variations in wind velocity due to meteorological or topographical conditions within the domain, are therefore not accounted for in this model.

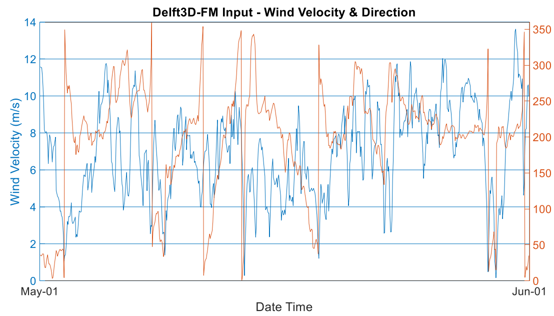

Figure 3. Hourly wind speed & direction (model inputs).

2) Boundary Conditions

The open (Southern) boundary of the hydrodynamic FLOW simulation was forced astronomically using the TPXO 7.2 Global Inverse Tidal Model. This model provides gridded estimates of tidal coefficients by interpolating between constituents confirmed by active tide gauge stations. This boundary provides the driving force [14] to generate V_d, the depth-averaged flow velocities (Figure 4).

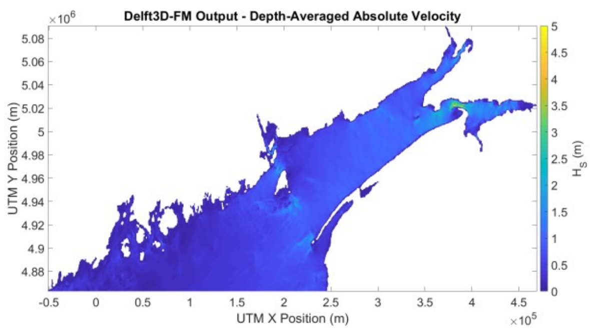

Figure 4. Delft3D-FM FLOW snapshot of V_d.

The open boundary of the phase-averaging SWAN (Simulating WAves Nearshore) simulation was set to Significant Wave Height (H_S) = 1m, Period (T) = 5s and Wave Direction (from) (H_{dir}) = 180°. This represents a moderately developed sea state in a deep area, that is not limited by fetch to the South [15]. These boundary conditions are then propagated into the model domain by the wind velocity inputs (Figure 5) to generate spatially-varying estimates of H_S.

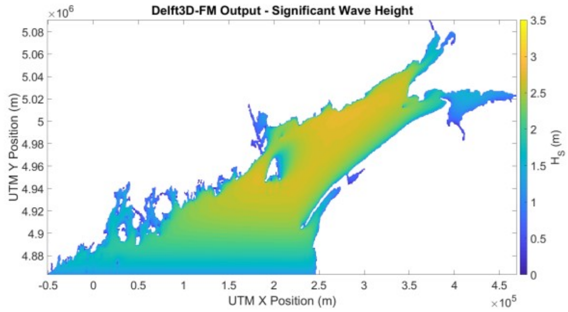

Figure 5. Delft3D-FM WAVE (SWAN) snapshot of H_S.

C. Calculating Operational Windows

1) Operational Constraints

In order to calculate an approximation for weather window occurrences and durations, it is necessary to input transit and safe working limitations as operational constraints. Table 1 shows example constraints for a maintenance operation, based on SME operational experience with work boats and marine contractors. The symbols (-) and (~) denote not applicable and spatially varying parameters respectively.

Table 1. Maintenance Operation Constraints

Limiting Parameter	Transit	Operation
Surface Flow Velocity (m/s)	3	1
Wind Velocity (m/s)	20	20
Significant Wave Height (m)	2	1
Vessel Max Transit Speed (m/s)	3	-
Water Depth (m)	3	15
Operational Duration (h)	~	3
Operational Frequency (per year)	24	12

It is assumed that because PLAT-I requires 15m water depth for successful deployment, depth during the operation itself will not be a constraint. Wind velocity is also not expected to be constraining, because at no point during the DHI dataset do the velocities come close to a conservative operational limits of 20m/s. However, the impact of the wind on wave growth will certainly be a limiting factor. The monthly maintenance operations will require return journeys, hence 24 total transit passages.

The Surface Flow Velocity (V_S) was calculated by splitting the data into 1m depth bins and assuming a 1/7th Power Law velocity profile for each depth-averaged velocity data point within the model domain (Equation 1)

$$\frac{V_b}{V_S} = \left(1 - \frac{d_b}{d}\right)^{\frac{1}{7}}$$

Equation 1

V_b is the velocity at the binned depth (d_b), with d being the maximum water depth. In this V_S is then iteratively calculated by increasing from the value of V_d in small increments until the abstract areas per second $A_{V_d d_b}$ (Equation 2), and $A_{V_b d_b}$ (Equation 3) are equal.

$$A_{V_d d_b} = \sum_{b=1}^{d} V_d \cdot d_b$$

Equation 2

$$A_{V_b d_b} = \sum_{b=1}^{d} V_b \cdot d_b = \sum_{b=1}^{d} V_S \cdot \left(1 - \frac{d_b}{d}\right)^{\frac{1}{7}} \cdot d_b$$

Equation 3

2) Path from Site to Port

An adequately equipped port is also required, from which to launch maintenance operations. Within the domain, several suitable ports have been identified (Figure 6).

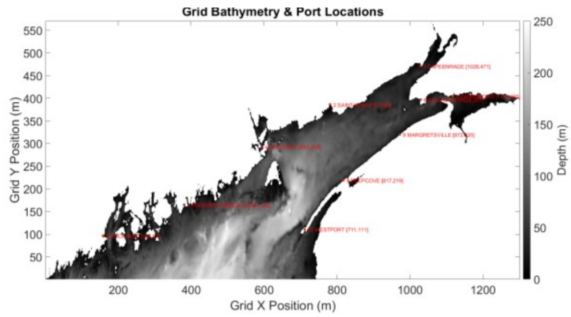

Figure 6. Port locations within the domain.

In order to estimate the transit distance and time for a marine operation, as well as the likely MetOcean conditions encountered, it is necessary to designate an efficient route from the nearest port to each point within the domain.

An A-Star (A*) Algorithm was employed to find the shortest heuristically weighted path between two valid points on the grid. Valid points were designated as a) not land, and b) deep enough to transit through (3m depth) The weighting/mobility, of the A* is the ease with which the algorithm will progress to the next point. The "greediness" of the algorithm was set to 2.5 for faster computation. Water depth and absolute distance between nodes was used as the heuristic weighting criteria to ensure that the path remained short and shallow, representing an efficient and sheltered route for vessels (Figure 7). At each grid cell node along the algorithm path, the depth-averaged flow velocity, and significant wave height were output for every hour of the simulation. The probability of the transit limits being exceeded at any single node along the transit route, and the operational limits being exceeded at the deployment site node, can then be estimated.

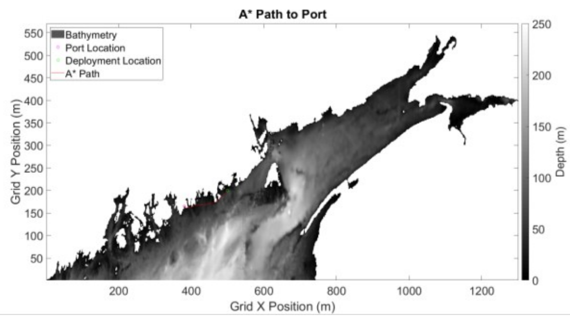

Figure 7. Example of an A* path from site to port.

3) *Neap Tide Identification – Flow Constraints*

In areas with potential for tidal energy development, an ever-present constriction upon marine operations is the tidal flow velocity. As per Table 1, maintenance operations will be unable to proceed in flow velocities >1m/s, and it will be unsafe to transit through flow velocities >3m/s. During fortnightly spring (stronger) tides, the daily period of accessibility is relatively short, as the flow velocity at site must remain below the operational thresholds for the duration of the marine operation (3h). Therefore, O&M is targeted to slack periods and planned to occur during neap (weaker) tides [16]. While this potentially does not leave many available hours within a month for O&M, the tides are a highly predictable resource [17]. This means that the length and timing of the neap slack periods can be predicted far in advance through harmonic analysis (if historic data is available), or in this case through the numerical modeling techniques presented. Using this method effectively means that the model Duration (D) is reduced from 744 hours (per month) to the number of hours during the fortnightly neap periods (D_n) where the flow speed remains below the operational threshold for the length of the required maintenance operation.

4) *Weibull Persistence Statistics – Wave Constraints*

Waves are not so easily predicted, and therefore a probabilistic method is required to estimate their impact on the success of marine operations. By extracting a time series of H_S at each node along the transit route, the probability of operational thresholds being exceeded at any point during transit can be calculated through a Weibull Persistence Method (WPM) [9], [10]. By applying a Weibull Fit to the probability of exceedance of the wave data, it is possible to identify the shape (k), scale (b) and location (X_0) parameters. The k parameter alters the shape of the distribution, such that it could take on the appearance of a bell curve, or exponentially tend towards zero or one. The scale parameter b focuses the density of the probability distribution into a smaller area. Finally, the location parameter shifts the distribution along the x-axis. It is defaulted to 0 and is only altered to provide a better fit to the raw probability of exceedance data. Having identified the Weibull Parameters k and b, the Weibull Probability of Exceedance (p_{wb}) can then be calculated (Equation 4).

$$p_{wb}(H_S > H_{Lim}) = e^{-\left(\frac{H_{Lim}-X_0}{b}\right)^k}$$

Equation 4

H_{Lim} is the threshold operational limit for significant wave height as per Table 1. P_{wb} allows for the calculation of the average length of an accessible wave window with that meets the operational constraints (T_{Av}) (Equation 5).

$$T_{Av} = p_{wb}(H_S > H_{Lim}) \cdot \frac{D}{N_\omega}$$

Equation 5

D is the model duration in hours and N_ω is the number of wave window occurrences within the modelled duration. For example, if a threshold operational limit was only exceeded twice separately during a month, then N_ω= 3. The probability that a normalised accessible window (X_i) will persist for longer than the average window duration (T_{Av}) is known as the Probability of Persistence (Equation 6). X_i is defined as the operational length requirement divided by T_{Av}.

$$p_{wb}(X_i > T_{Av}) = e^{-C_{Acc} \cdot (X_i)^{\alpha_{Acc}}}$$

Equation 6

C_{Acc} is the occurrence of accessible wave conditions as derived from the Weibull distribution shape (Equation 7) and α_{Acc} is the relationship between the mean significant wave height value ($\bar{H}$) and the threshold operation value (H_{Lim}) assuming a linear correlation characteristic (Equation 8) [18].

$$C_{Acc} = \left[\Gamma\left(1 + \frac{1}{\alpha_{Acc}}\right)\right]^{\alpha_{Acc}}$$

Equation 7

$$\alpha_{Acc} = 0.267\gamma\left(\frac{H_{Lim}}{\bar{H}}\right)^{-0.4}$$

Equation 8

The γ coefficient (Equation 9) and $\bar{H}$ (Equation 10) are both derived from the Weibull distribution shape, scale and location parameters.

$$\gamma = k + \frac{1.8X_0}{\bar{H} - X_0}$$

Equation 9

$$\bar{H} = b \cdot \Gamma\left(1 + \frac{1}{k}\right) + X_0$$

Equation 10

Combining the probabilities of Weibull Exceedance and Persistence allows for calculation of the occurrence of a weather window with both specified MetOcean limits and required duration (Equation 11).

$$p_{wb}(T > T_{Av}) = p_{wb}(X_i > T_{Av}) \cdot \left(1 - p_{wb}(H_S > H_{Lim})\right)$$

Equation 11

D. *Levelised Cost of Energy*

1) *Access & Waiting Hours*

The Weibull distribution can be utilised to not only estimate the likelihood of a weather window occurring, but also the number of access hours (N_{Acc}) in a given duration that such windows will occur for (Equation 12), and how long it is likely that an operation will have to wait (N_{Wait}) before a weather window occurs (Equation 13).

$$N_{Acc} = D \cdot p_{wb}(T > T_{Av})$$

Equation 12

$$N_{Wait} = \frac{\left(D - (N_{Acc} \cdot T_{Av})\right)}{N_{Acc}}$$

Equation 13

The Weibull Persistence Method is well suited for this application, due to its computational simplicity compared to time-based methods [19]. The equations described here can be performed relatively quickly over a large number of grid points, without needing to iterate through the potentially thousands of generated time series for different operation start and end times. Further details of this assessment are given in [3], [20]. Figure 8demonstrates the spatial variation in waiting hours, where the areas of highest flow and wave, furthest from port have the longest waiting hours.

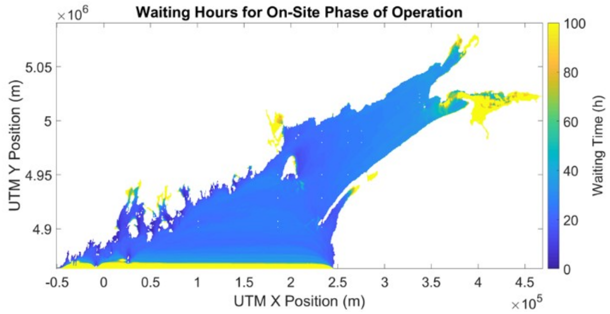

Figure 8. MetOcean induced waiting hours.

2) Power Generation

Power Generated (P_G) was calculated by utilising a power-weighted average velocity over the swept area of the turbines, and the power curves of the SCHOTTEL Hydro 4m rotors [21] (Figure 9).

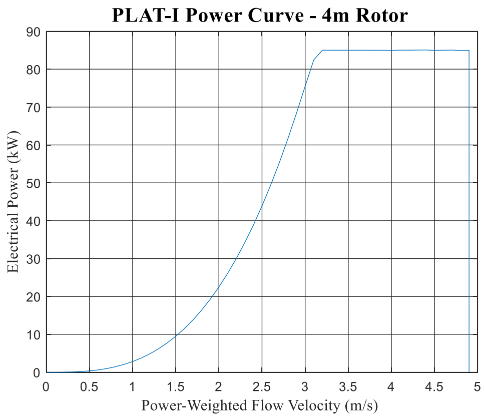

Figure 9. PLAT-I SIT 4m rotor power curve.

An estimate of flow velocities swept by the rotors assuming a 4m hub depth, was calculated using the 1/7th Law Profile. The depth-varying binned velocities V_b were then input into Equation 14 to calculate the power-weighted average velocity (V_P).

$$V_P = \left[\frac{1}{A} \cdot \sum_{b=1}^{n} V_b^3 \cdot A_b\right]^{\frac{1}{3}}$$

Equation 14

A is the total swept area of the rotors, and A_b is the amount of swept area contained within each depth bin. An estimate of P_G is inferred from the rotor performance characteristics and V_P at each node and time step of the model.

3) Electrical Losses

Electrical Power Losses (P_L) were calculated as a function of distance to shore, power generated and the transmission parameters [23] given below in Table 2. Grid connection points were designated as the moderately sized ports established within the domain.

The cabling route to shore was calculated through the A* algorithm used to estimate a path to port. This means that the cabling route is primarily short and in shallower water, but does not take the shortest path to land.

Table 2. Electrical Transmission Parameters

Transmission Parameter	Value
Generation Voltage (V)	440
Export Cable Voltage (V)	6600
Grid Voltage (V)	13800
PLAT-I Rated Power (kW)	280
Export Cable Cross Section (mm^2)	10
Export Cable Resistance (ohm/km)	0.99
Water Temperature (°C)	8
De-rating (%)	107
Power Factor (%)	95
Transformer Efficiency (%)	96
Switchgear Efficiency (%)	99

4) Idealized Energy Delivered

The idealized energy delivered (E_I) at each node during the entire model duration was calculated through Equation 15. Figure 10 demonstrates the spatial variation in idealized energy delivered, assuming no downtime.

$$E_M = \sum_{t=1}^{D} (P_{G_t} - P_{L_t})$$

Equation 15

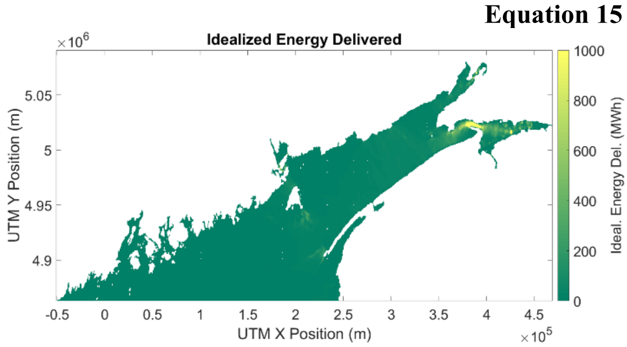

Figure 10. Idealized annual energy delivered.

5) Downtime

Total downtime during the deployment was approximated as a total of three calculation processes:

1. Downtime due to failure of planned marine operations. This is expected to be negligible, since rearranging the operation for a few days or even a month is unlikely to incur much loss of power generation if the maintenance is non-essential.

2. Downtime due to failure of unplanned marine operations. This will be highly sensitive to the selected deployment location. If faults/damage occurs, or if an unexpected but urgent repair is required, then there will be a period of downtime until the corrective O&M can be completed. MetOcean conditions will affect the viability of marine operations.

3. Downtime due to extreme MetOcean conditions. Again, this will be highly sensitive to the deployment location, and thus will vary spatially. If for safety or to prevent damage to components, power generation must be ceased repeatedly, then this will have an impact upon the downtime and total amount of power that can be exported.

Because the approach used to calculate the number of waiting hours is probabilistic, the amount of hours lost to downtime must also be expressed probabilistically (rather than designating which specific hours throughout the year are lost). This means that the probability of generating hours being lost to downtime (p_D) can be expressed by the following formula (Equation 16):

$$p_D = \frac{N_{Wait}}{D} + p_{wb}(H_S > H_{Lim})$$

Equation 16

The amount of energy actually delivered to grid (ED) is then calculated through Equation 17 and shown to vary spatially as per Figure 11.

$$E_D = (1 - p_D) \cdot E_M$$

Equation 17

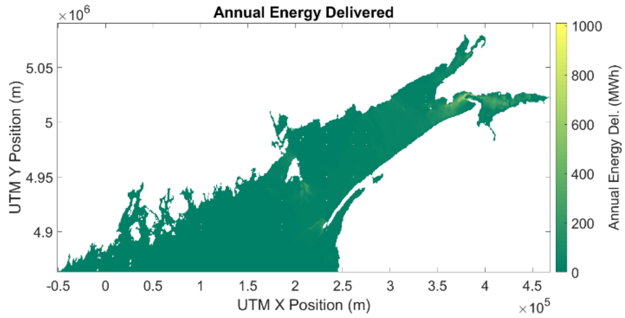

Figure 11. Actual annual energy delivered.

6) Economic Assignment

A successful marine operation will incur the cost estimates A-D given in **Error! Reference source not found.**. However, planned marine operations rarely occur without delay or re-arrangement, and therefore standby costs (E) are incurred.

The overall cost of rescheduled operations was calculated through a standard Standby Contract Method which incurs a vessel standby (E) and staff cost (B) each day until the operation is successful. For infrequent but essential marine operations, this option is the most commonly used, despite the risk of a potentially prolonged and costly standby period. In this paper, the standby period will be calculated through the WPM for waiting hours/days.

Table 3. Maintenance Operation Costs

Aspect of Operation	Cost ($ USD)
A: Vessel Hire (per day)	4500
B: 2x Specialist Staff (per day)	1000
C: Vessel Transit (per km)	100
D: Vessel Running (per hour)	500
E: Vessel Standby (per day)	2500

7) LCoE

LCoE was calculated through use of Equation 18:

$$LCoE = \frac{\sum_{t=1}^{n} \frac{I_t + M_t + D_t}{(1+r)^t}}{\sum_{t=1}^{n} \frac{AEP_t}{(1+r)^t}}$$

Equation 18

Where n is the total number of years (t) of which the tidal development will occur (in this paper, 10 years), r is the discount rate (in this paper, 5% is applied). I_t is the initial costs of each year, such as development and installation operations. M_t is the cost of maintenance operations, or operational expenditure. D_t is the shutdown or decommissioning costs of each year. AEP_t is the annual energy production in MWh for each year.

The initial and decommissioning costs only come into play in the first and final year respectively. In this instance, it is assumed that installation and decommissioning operations have the same metocean constraints as a maintenance operation, and thus are subject to the same increases in cost.

III. Results

A. Optimum Site Selection

1) Idealized Energy Delivered Approach

If MetOcean conditions are not accounted for (no downtime, and no standby costs), then areas of highest resource are shown to have the lowest LCoE as per Figure 12. The most evident low LCoE locations are shown to be areas that have already been developed into tidal energy deployment hubs, such as FORCE. Areas of bathymetric constriction such as headlands and narrow inlets also show low LCoE due to their high flow speeds and proximity to shore.

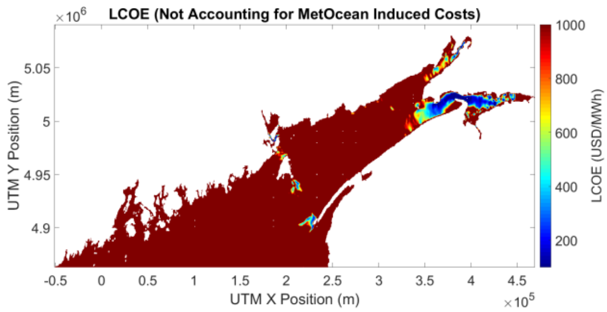

Figure 12. LCoE calculated through idealized approach.

2) Holistic LCoE Approach

Taking a more holistic approach that accounts for MetOcean induced costs shows that areas of moderate resource are the most economically viable (Figure 13). However, the magnitude of profitability (higher LCoE) is drastically reduced now that the negative financial impacts of constraining MetOcean parameters has been incorporated into the LCoE equation.

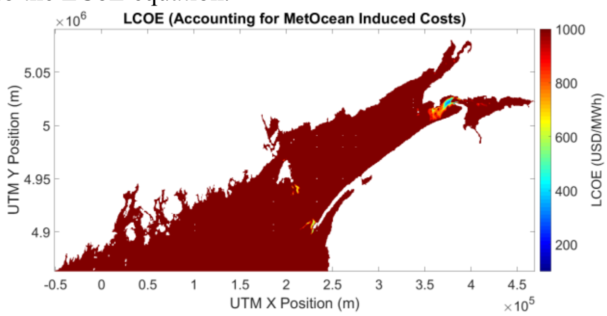

Figure 13. LCoE calculated through holistic approach.

Importantly, the very highest resource locations show a much higher LCoE, due to the constraining effect of the tide. In areas such as FORCE and other narrow inlets to the North of the domain, the number of available hours for operations due to the tide is so few, that when combined with even relatively sheltered wave conditions, waiting times and standby costs increase such that the site becomes economically unviable.

The lower flow speed areas to the West of FORCE, or at Grand Passage to the South of the Digby Peninsula, are shown to have the lowest LCoE when a more holistic approach is applied. Given the tidal energy sector's relative immaturity and need for frequent marine operations, pursuing these "moderate-flow, low operating cost" locations is the prudent choice, over more conventional "high-flow, high revenue" sites.

Choosing sites more holistically will reduce the barriers to entry; allowing more projects to proceed and therefore providing the industry with experience and learning. This would allow for the development several positive impacts. An incremental increase in the size of turbines, such that even more power could be generated per required operation. Array deployments could occur, and maintenance trips combined to allow for a reduced time per operation per platform. The tidal developer would also learn the dominant issues that demand such frequent operations; improving certain components or processes could lead to less required operations, meaning that the negatives of MetOcean impacts on LCOE would be reduced, or even mitigated.

B. Discussion

1) Limitations of Methodology

It was acknowledged that a purely frequency-based approach was not appropriate for the estimation of tidal flow-based weather windows. Due to the small number of persistently low-flow windows, the operations will always be constrained to a few hours within the month (the neap periods). Hence the augmented Weibull Persistence Method, that used the tidal constraints to alter the duration over which the random wave constraining probability was applied. This proved to be computationally efficient and the results are shown to be highly informative to the site assessment of tidal energy deployments, giving a reasonable first-pass approximation of the likely operational time and related costs.

However, it is worth noting that daylight hours and other practical limitations are not yet taken into account, so the actual number of waiting hours and associated costs are likely to be higher due to decreased access hours. Thus, the estimates presented in this paper are likely to be optimistic.

No attempt to quantify the impacts of array deployments on LCoE has been made of yet. Four PLAT-I devices could conceivably be places in each grid cell, increasing revenue by a factor of 4, but with operational costs not necessarily increasing in the same linear fashion. Combining operations could potentially decrease the relevance of metocean parameters on cost, meaning that high-resource sites are again seen to be the most viable. Conversely, if operation sharing cannot be achieved, then the increased number of required operations would make the moderate-flow, sheltered sites all the more desirable.

2) Modelling Constraints

The numerical modelling techniques utilised for this paper are not designed to be a perfect recreation of complex natural phenomena. Their purpose is to allow a tidal developer to make an informed initial choice between potential deployment locations; providing quantifiable inputs to a decision that was previously either not considered, or burdened with a lack of data and high uncertainties. This is particularly important when targeting remote or lesser known sites.

That being said, the model is limited in several ways. Currently, the grid cell resolution is low, only one vertical layer is applied, and a $1/7^{th}$ power law profile was assumed across the domain. Increased realism would be achieved with more layers, allowing for the increased resolution of turbulence, boundary layer interactions and interactions of waves with flow. However, with this would come a huge increase in computational complexity and time; the trade-off between accuracy and applicability must be considered.

While the model has been calibrated against several discrete data points, the application of the calibrated model parameters constantly across the whole domain is potentially a source of error. For example, it is unlikely that the eddy diffusivity or bed friction is uniform, as in reality variations in bed type and even marine vegetation would alter these parameters. However, this is an inherent but unavoidable model limitation. The cost of gathering detailed spatially varying data for calibration would far outweigh the increase in model accuracy that could potentially be achieved.

IV. Conclusions

The impacts of the MetOcean parameters flow velocity and significant wave height on tidal energy operational costs have been quantified. This allowed for the development of a more holistic site selection methodology, which incorporates these impacts as well as the more conventional revenue-based selection criteria.

Choosing a sheltered, moderate-resource location is seen to be the most economically viable. Incorporating MetOcean impacts early on in the planning stage will give a better estimation of project lifetime costs and ensure that these expenses are factored into the site selection methodology, such that an optimum location is chosen for detailed investigation or final deployment.

Acknowledgments

The authors wish to acknowledge the companies and funding bodies who have enabled the collection and interrogation of the data used in this paper, as well as allowing for its publication. Sustainable Marine Energy Ltd. have provided integral data, expertise and financial support. The software developers at Delft Deltares, GEBCO and DHI have developed essential modelling tools and data. The Industrial Doctoral Centre for Offshore Renewable Energy (IDCORE) and its contributing funding bodies have provided the authors with facilities and financial backing, without which this paper could not have been produced.

REFERENCES

[1] R. Vennell, “Estimating the power potential of tidal currents and the impact of power extraction on flow speeds,” *Renew. Energy*, vol. 36, no. 12, pp. 3558–3565, 2011.

[2] R. Ahmadian and R. A. Falconer, “Assessment of array shape of tidal stream turbines on hydro-environmental impacts and power output,” *Renew. Energy*, vol. 44, pp. 318–327, 2012.

[3] J. Mcdowell, P. Jeffcoate, T. Bruce, and L. Johanning, “Numerically Modelling the Spatial Distribution of Weather Windows : Improving the Site Selection Methodology for Floating Tidal Platforms,” 2018.

[4] P. Jeffcoate, J. Mcdowell, and N. Cresswell, “Floating Tidal Energy Site Assessment Techniques for Coastal and Island Communities,” 2018.

[5] Deltares systems, “Delft3D-FLOW, User Manual,” pp. 1–684, 2014.

[6] T. Swan, “USER MANUAL SWAN - Cycle III version 41.01A,” *Cycle*, p. 126, 2009.

[7] G. Egbert and L. Erofeeva, “TPXO global and local models,” pp. 2–3.

[8] J. D. H. Wiseman and C. D. Ovey, “The general bathymetric chart of the oceans,” *Deep Sea Res.*, vol. 2, no. 4, pp. 269–273, 2008.

[9] C. Frost, D. Findlay, E. Macpherson, P. Sayer, and L. Johanning, “A model to map levelised cost of energy for wave energy projects,” *Ocean Eng.*, vol. 149, no. January 2017, pp. 438–451, 2017.

[10] R. T. Walker, J. Van Nieuwkoop-Mccall, L. Johanning, and R. J. Parkinson, “Calculating weather windows: Application to transit, installation and the implications on deployment success,” *Ocean Eng.*, vol. 68, pp. 88–101, 2013.

[11] F. Achete, “Morphodynamics of the Ameland Bornrif,” 2011.

[12] T. A. D. Davey, V. Venugopal, F. Girard, H. C. M. Smith, G. H. Smith, J. Lawrence, L. Cavaleri, L. Bertotti, M. Prevosto, and B. Holmes, “D2.7 Protocols for wave and tidal resource assessment,” *EquiMar Protoc.*, 2010.

[13] F. Schlütter, O. S. Petersen, and L. Nyborg, “Resource Mapping of Wave Energy Production in Europe,” pp. 1–9, 2015.

[14] G. D. Egbert and S. Y. Erofeeva, “Efficient inverse modeling of barotropic ocean tides,” *J. Atmos. Ocean. Technol.*, vol. 19, no. 2, pp. 183–204, 2002.

[15] A. Cooper and R. Mulligan, “Application of a Spectral Wave Model to Assess Breakwater Configurations at a Small Craft Harbour on Lake Ontario,” *J. Mar. Sci. Eng.*, vol. 4, no. 3, p. 46, 2016.

[16] M. Morandeau, R. T. Walker, R. Argall, and R. F. Nicholls-Lee, “Optimisation of marine energy installation operations,” *Int. J. Mar. Energy*, vol. 3–4, pp. 14–26, 2013.

[17] Daniel Codiga, “"UTide" Unified Tidal Analysis and Prediction Functions - File Exchange - MATLAB Central,” 2017.

[18] T. Stallard, J. F. Dhedin, S. Saviot, and C. Noguera, “D7.4.1 Procedures for estimating sit accessibility & D7.4.2 Appraisal of implications of site accessibility,” *EquiMar Protoc.*, 2010.

[19] T. Stallard and P. K. Stansby, “D7.3.1 Support Structures for Arrays of Wave Energy Devices,” *EquiMar Protoc.*, 2009.

[20] J. Mcdowell, T. Bruce, and P. L. Johanning, “Numerical Modelling of the Spatial Distribution of Revenue and O & M Costs for Floating Tidal Platforms,” 2017.

[21] P. Jeffcoate, R. Starzmann, B. Elsaesser, S. Scholl, and S. Bischoff, “Field measurements of a full scale tidal turbine,” *Int. J. Mar. Energy*, vol. 12, pp. 3–20, 2015.

[22] C. Legrand, Black and Veatch, and Emec, *Assessment of Tidal Energy Resource*. 2009.

[23] H. Brakelmann, “Loss determination for long three-phase high-voltage submarine cables,” *Eur. Trans. Electr. Power*, vol. 13, no. 3, pp. 193–197, 2003.